Available online at www.sciencedirect.com
SCIENCE DIRECT
ELSEVIER
Journal of Nuclear Materials 329–333 (2004) 257–262
journal of nuclear materials
www.elsevier.com/locate/jnucmat

Materials design data for reduced activation martensitic steel type EUROFER

A.-A.F. Tavassoli [a,*], A. Alamo [b], L. Bedel [c], L. Forest [b], J.-M. Gentzbittel [c], J.-W. Rensman [d], E. Diegele [e], R. Lindau [e], M. Schirra [e], R. Schmitt [e], H.C. Schneider [e], C. Petersen [e], A.-M. Lancha [f], P. Fernandez [f], G. Filacchioni [g], M.F. Maday [g], K. Mergia [h], N. Boukos [h], Baluc [i], P. Spätig [i], E. Alves [j], E. Lucon [k]

[a] *DMN/Dir, Commissariat à l'Energie Atomique, CEA/Saclay, 91191 Gif sur Yvette, cedex, France*
[b] *Commissariat à l'Energie Atomique, CEA/Saclay, 91191 Gif sur Yvette, cedex, France*
[c] *Commissariat à l'Energie Atomique, CEA/Grenoble, 17, rue des martyrs, 38054 Grenoble, cedex 9, France*
[d] *NRG Petten, Westerduinweg 3, P.O. Box 25, 1755 ZG, Petten, The Netherlands*
[e] *Forschungszentrum Karlsruhe, Postfach 3460, Karlsruhe, D-76021, Germany*
[f] *CIEMAT Fusion Association, Avenida Complutense 22, 28040 Madrid, Spain*
[g] *ENEA CR Cassaccia, 2400-00100 Rome, Italy*
[h] *N.C.S.R. 'Demokritos', Institute of Nuclear Techology and Radiation Protection, 153 10 Ag. Paraskevi Attikis, Greece*
[i] *CRPP-EPFL, Fusion Technology Materials, ODGA/105, 5232 Villigen-PSI, Switzerland*
[j] *Instituto Technologico e Nuclear, Estrada Nacional 10, P-2686-953 Sacavem, Portugal*
[k] *SCK• CEN, Boeretang 200, MOL, B-2400, Belgium*

Abstract

Materials design limits derived so far from the data generated in Europe for the reduced activation ferritic/martensitic (RAFM) steel type Eurofer are presented. These data address the short-term needs of the ITER Test Blanket Modules and a DEMOnstration fusion reactor. Products tested include plates, bars, tubes, TIG and EB welds, as well as powder consolidated blocks and solid–solid HIP joints. Effects of thermal ageing and low dose neutron irradiation are also included. Results are sorted and screened according to design code requirements before being introduced in reference databases. From the physical properties databases, variations of magnetic properties, modulus of elasticity, density, thermal conductivity, thermal diffusivity, specific heat, mean and instantaneous linear coefficients of thermal expansion versus temperature are derived. From the tensile and creep properties databases design allowable stresses are derived. From the instrumented Charpy impact and fracture toughness databases, ductile to brittle transition temperature, toughness and behavior of materials in different fracture modes are evaluated. From the fatigue database, total strain range versus number of cycles to failure curves are plotted and used to derive fatigue design curves. Cyclic curves are also derived and compared with monotonic hardening curves. Finally, irradiated and aged materials data are compared to ensure that the safety margins incorporated in unirradiated design limits are not exceeded.

1. Introduction

ITER detailed design report [1] is supported by an interim structural design criteria (IISDC) [2] where materials physical and mechanical properties are

* Corresponding author. Tel.: +33-1 6908 6021; fax: +33-1 6908 8070.
E-mail address: tavassoli@cea.fr (A.-A.F. Tavassoli).

0022-3115/$ - see front matter
doi:10.1016/j.jnucmat.2004.04.020

presented in a document similar to that of the 'Appendix A: Materials data and Analysis' in the RCC-MR [3]. However, ITER documents are written mainly for austenitic stainless steels [4,5] and concern operations at low temperatures and low neutron doses. They do not include at present rules and data for reduced activation ferritic/martensitic steels (RAFM steels), the primary structural material considered for ITER Test Blanket Modules (ITBM) and a DEMOnstration reactor. While the time-schedule for development of Demo interim structural design criteria (DISDC) is relatively long, that of the ITBM is short and concurrent with ITER [6] and there is hence the need for an interim RAFM Appendix A document.

It is recalled that RAFM steels are alloys whose main compositions are derived from the conventional modified 9Cr–1Mo steel [7], but with the high activation elements, such as Mo and Nb, replaced by their equivalent low activation elements (e.g. W, V and Ta). The presence of high activation residual elements is also kept as low as possible. In a previous report, materials properties data for F82H, an RAFM steel produced in Japan [8] and tested under the IEA Fusion materials collaborative agreement, were reported [9], here those of the Eurofer, a steel produced in Europe [10], are reported.

2. Procedures

Procedures used for Eurofer steel data collection and analyses are similar to those reported for F82H steel [9,11]. Continued attention is paid to the quality of data to ensure that all materials properties data collected and used are fully traceable and are obtained and analysed according to internationally accepted procedures. Data obtained from tests on small or non-standard specimens are only used for comparison or substantiation of conclusions drawn from tests on standard specimens.

3. Materials

Several 2000 kg heats of Eurofer steel have been produced for EU by Böhler/Austria. Table 1 shows the chemical composition specification used for these orders. For comparison, that of the F82H steel is also given in Table 1. Products received were in the form of plates, bars, tubes and wires. They were all referenced in one EU laboratory and then dispatched to the others for testing. EB and TIG joints, as well as the HIP products, were also made in one EU laboratory for all.

The final heat treatment applied to products varied slightly according to their type and size. For plates it consisted of:

Table 1
Specified chemical compositions of Eurofer and F82H steels [target values]

Elements	F82H steel	Eurofer 97 steel
Cr	7.7	8.5–9.5 [9.0]
C	0.09	0.09–0.12 [0.11]
Mn	0.16	0.20–0.60 [0.40]
P	0.002	<0.005
S	0.002	<0.005
V	0.16	0.15–0.25
B	0.0002	<0.001
N_2	0.006	0.015–0.045 [0.030]
O_2	(0.01)	<0.01
W	1.94	1.0–1.2 [1.1]
Ta	0.02	0.06–0.09
Ti	100 ppm	<0.01 (100 ppm)
Nb	1 ppm	[<10 ppm]
Mo	30 ppm	[<50 ppm]
Ni	200 ppm	[<50 ppm]
Cu	100 ppm	[<50 ppm]
Al	30 ppm	[<100 ppm]
Si	1100 ppm	<500 ppm
Co	50 ppm	[<50 ppm]
Sn	(<20 ppm)	As + Sn + Sb + Zr <100 ppm
As	(<50 ppm)	As + Sn + Sb + Zr <100 ppm

Normalising at 980 °C for 27–30 min followed by air cooling.

Tempering at 760 °C for 90 min followed by air-cooling.

Welded and HIP joints were all post heat treated. In addition to check analyses and microstructural examinations at all EU laboratories for verification of homogeneity of products, in depth chemical analyses of products were also made for traces of rare active elements like uranium. No abnormalities were found.

4. Results

To save space in this paper many tables and figures are omitted. For full description of results the reader is referred to the Appendix A report [12].

4.1. Physical properties

Not all the physical properties of Eurofer steel have been measured as yet. Currently data on specific heat, thermal diffusivity and thermal conductivity properties are available. Estimated values of the Young's modulus and mean coefficient of thermal expansion from tension and fatigue tests are also available.

An example of the physical properties results obtained is shown in Fig. 1. Also shown in this figure are values for F82H and conventional 9Cr–1Mo steels. It can be seen that the differences between the properties of

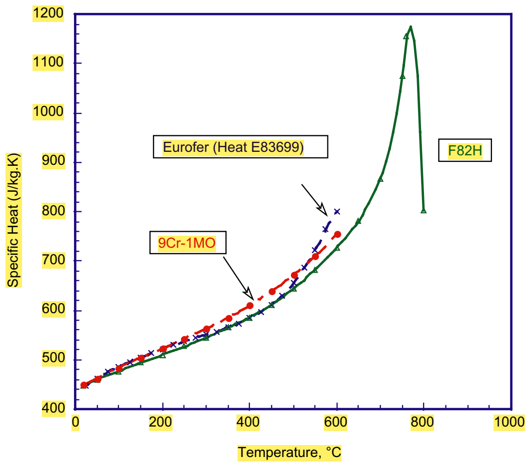

Fig. 1. Comparison of the specific heat values of the Eurofer steel with those of the conventional 9Cr–1Mo steel and the reduced activation F82H steel.

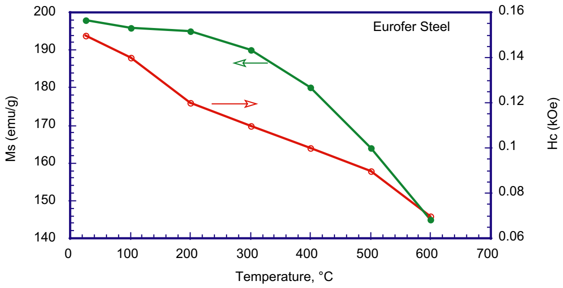

Fig. 2. Plot of mass induced saturation magnetization and coercive force versus test temperature (Demokritos data).

the three steels are small. This observation can help during the preliminary analyses, where one can use the results of other two materials for missing Eurofer data.

Fig. 2 shows a plot of variations of saturation magnetization and coercive force versus temperature for Eurofer steel. The recorded saturation magnetization values are similar to those obtained for the F82H steel, but the coercive force values are different. Additional tests are proposed on both alloys.

4.2. Tensile properties

Several tension tests have been carried out in EU laboratories on specimens taken from various Eurofer steel products in different orientations, with and without thermal ageing. The database constituted from these tests allows a reliable determination of stress intensity criterion, S_m, at temperatures up to 700 °C (Table 2).

Results from tests on irradiated materials, however, are still coming in, as are results from tests on the welded and HIPed joints. Figs. 3 and 4, nevertheless, show that both welding and irradiation increase strength, and hence do not affect the values of S_m reported in Table 2.

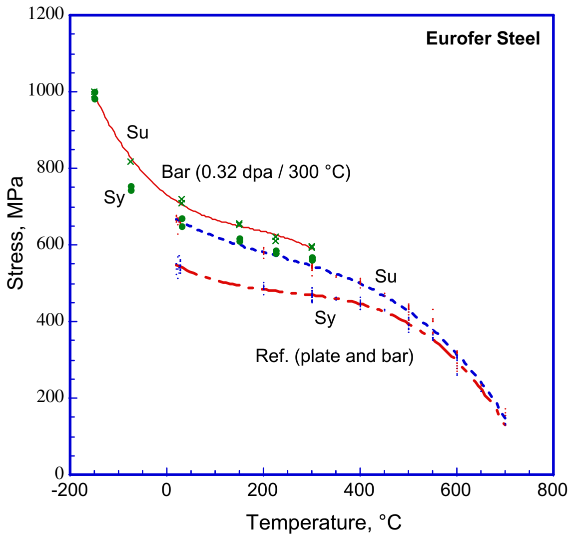

Fig. 3. Effect of irradiation on tensile properties of Eurofer steel (irr. data from SCK).

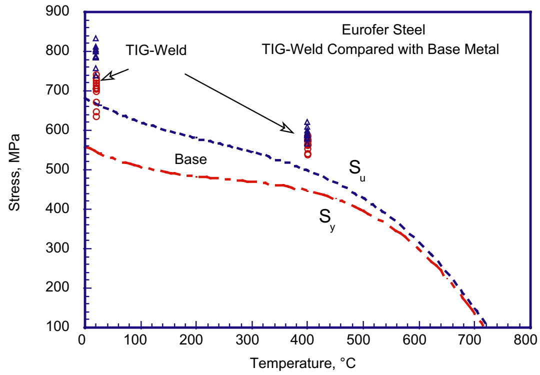

Fig. 4. Comparison of Eurofer TIG weld tensile properties with average base metal curves (CEA TIG data).

Table 2
S_m for Eurofer steel at temperatures 20 °C through 700 °C

Temperature °C	20	100	200	250	300	350	400	450	500	550	600	650	700
S_m (MPa)	207	192	180	174	169	162	154	145	132	117	98	74	46

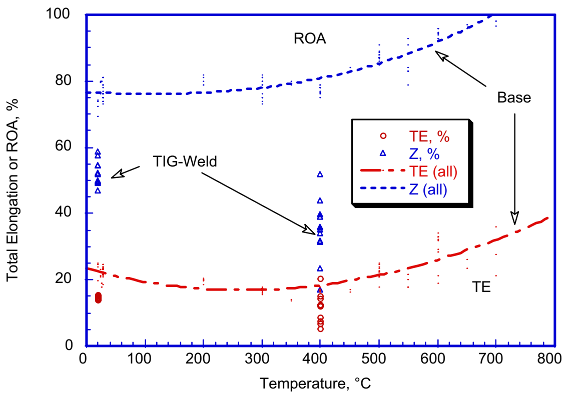

Fig. 5. Comparison of total elongation and reduction of area of Eurofer TIG weld joint and base metal (CEA TIG data).

Notice that this may not be the case for powder HIPed products, where fast cooling of large sections may not be possible.

Total tensile elongation of Eurofer steel versus test temperature remains above 10%, except in welded joints, where values as low as 1% are observed, as seen in Fig. 5. The reduction of area of base metal and welded joints remain higher than about 20%. The uniform elongation of Eurofer steel decreases from about 5% at room temperature to about 1% at 550 °C before increasing again at higher temperatures.

4.3. Creep properties

The creep database of Eurofer steel is reasonably good, with testing times of several experiments exceeding 10 000 h. Relevant master creep curves, based on equivalence of time and temperature, have been built from isothermal creep rupture, time to 1% deformation and time to the onset of tertiary creep results. A good correlation is obtained between the plots derived from the master curves and the experimental data.

Using the above master curves various time dependent properties have been derived. Table 3 shows that the values of S_t for Eurofer, are governed by 2/3 of the minimum stress to rupture criterion.

4.4. Fatigue properties

Fatigue database of Eurofer is still inadequate for detailed analysis. In addition, the data analysis is made further difficult due to the evolution of microstructure and stresses during fatigue testing of F/M steels. For instance, the hysteresis loop during isothermal strain-controlled fatigue testing at 1.5% total strain range, shows not only a reduction in the maximum stresses in tension and compression sides of the cycles but also a shift of the mean stress to the compressive side.

Harmonising a definition for N_r (N50 or N25) and then deducing the half-life stress values, cyclic fatigue curves have been plotted and compared with the monotonic hardening curves, as shown in Fig. 6. Here, the dynamic modulus of elasticity is used for determination of elastic component of monotonic and cyclic

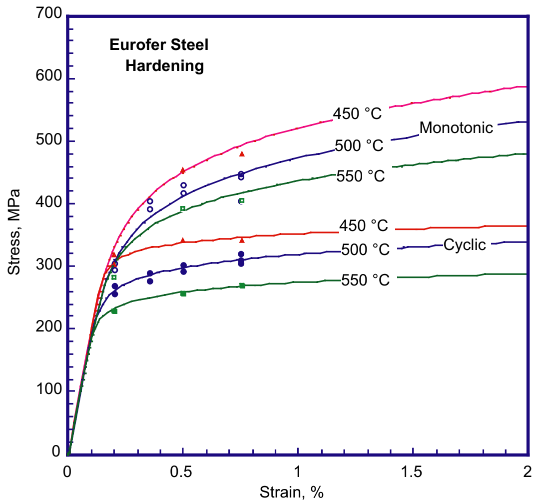

Fig. 6. Comparison of monotonic and cyclic curves using dynamic modulus (CIEMAT & ENEA data).

Table 3
Values of S_t (MPa) for temperature 425–675 °C

Time (h)	425 °C	450 °C	475 °C	500 °C	525 °C	550 °C	575 °C	600 °C	625 °C	650 °C	675 °C
10	290	265	240	216	192	169	147	126	105	85	66
30	279	254	229	204	181	158	136	115	94	74	55
100	267	242	217	192	169	146	124	103	82	63	44
300	256	231	206	181	158	135	113	92	72	52	33
1000	245	219	194	170	146	123	102	81	60	41	22
3000	234	208	183	159	136	113	91	70	50	31	12
10 000	223	197	172	148	124	102	80	59	39	20	
30 000	213	187	162	137	114	92	70	49	29	10	
100 000	201	176	150	126	103	81	59	39	19		
300 000	191	166	140	116	93	71	50	29	10		

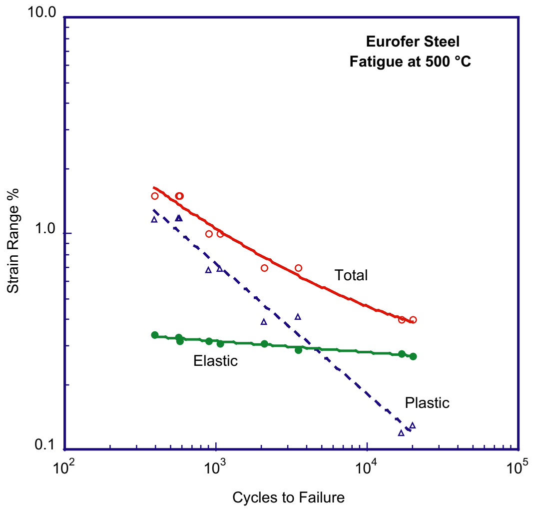

Fig. 7. Low cycle fatigue curve of Eurofer steel. Curves fitted to the total strain range (Langer) and elastic and plastic components (Manson–Coffin), (CIEMAT data).

curves. The conventional strain range versus number of cycles to rupture plots are shown in Fig. 7.

4.5. Impact toughness

Standard and small specimen impact tests have been carried out on all Eurofer products in the as-received, aged, welded and HIPed states. In all cases the ductile to brittle transition temperature is well below the room temperature and often equal or less than −50 °C. Fig. 8 shows an example of the results obtained for bar and solid–solid HIP joints.

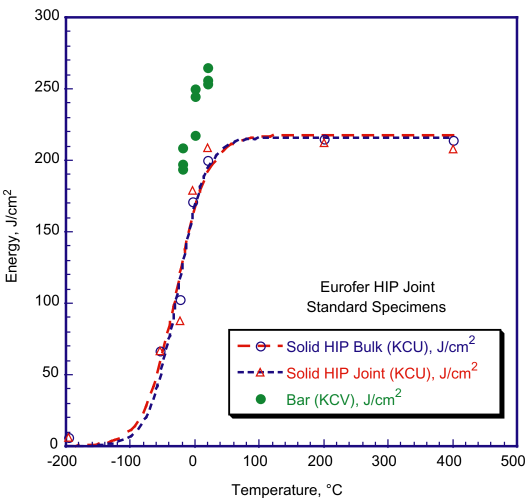

Fig. 8. Impact toughness of Eurofer solid HIP product, compared with the as-received metal (standard V and U notch specimens), (CEA data).

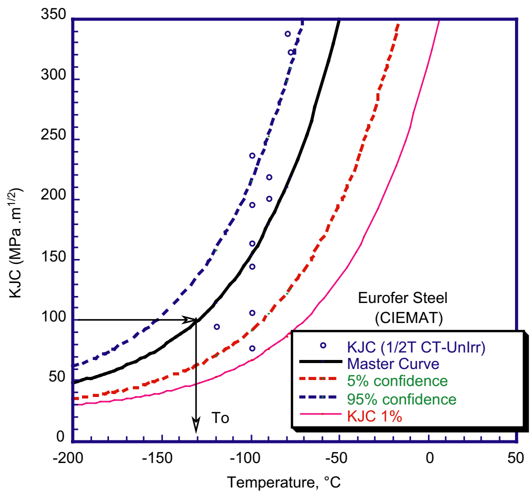

Fig. 9. Fracture toughness data of Eurofer steel (1/2T CT specimen results), (CIEMAT data).

The results on irradiated materials are still coming in but confirm a significant embrittlement at irradiation temperatures less than about 300 °C, as also observed on F82H steel.

4.6. Fracture toughness

Fracture toughness of Eurofer steel has been measured using CT and pre-cracked Charpy specimens. Harmonisation of results and evaluation procedures are under way.

Fig. 9 shows the master curve approach used for CT specimens tested in unirradiated condition ($T_0 = -130$ °C). The equation describing the med. curve is:

$$\text{KJC med.}(1T) = 30 + 70\exp(0.019(T - T_0))$$

Limited results available show a significant shift in T_0 after irradiation, e.g. to above room temperature after 2.7 dpa at 60 °C.

5. Conclusions

Eurofer steel data base constitution is proceeding well. Most of the information needed for ITER test blanket module design and preliminary design of a DEMOnstration reactor are now available. The properties recorded are in general similar to those of the F82H steel.

Acknowledgements

The results used in this work come mainly from the work done in the European laboratories.

The authors wish to express their gratitude to the European Union and EFDA for their financial and technical support.

References

[1] ITER detailed design report, ITER JCT, Garching JWS, Germany, 2001.
[2] P. Smith (Ed.), ITER Interim Structural Design Criteria (IISDC), Draft 5, doc. No. S74 RE 2 96-06-18 W 1.1, ITER, ITER JCT, 1996.
[3] RCC-MR 'Règles de Conception et de Construction des Matériels Mécaniques des îlots nucléaires RNR', Tomes, I et II, AFCEN, édition, 1993.
[4] A.-A.F. Tavassoli, Fusion Eng. Design 29 (1995) 371.
[5] A.-A.F. Tavassoli, F. Touboul, J. Nucl. Mater. 233–237 (1996) 51.
[6] A.R. Raffray, M. Akiba, V. Chuyanov, L. Giancarli, S. Malang, J. Nucl. Mater. 307–311 (2002) 21.
[7] J. Waering, A.-A.F. Tavassoli, Assessment of Martensitic Steels for Advanced Fusion Reactors, in: S.V. Möller, J.D. Riera, (Eds.), Transactions of the 13th International Conference in Structural Mechanics in Reactor Technology, Porto Alegre, Brazil, Universidade Federal do Rio Grande du Sul (UFRGS), 13–18 August 1995, Division E, p. 563.
[8] K. Shiba, Report of JAERI-Tech-97-038, JAERI, Tokyo, Japan, 1998.
[9] A.-A.F. Tavassoli, J.W. Rensman, M. Schirra, K. Shiba, Fusion Eng. Design 61&62 (2002) 617.
[10] R. Lindau, M. Schirra, Fusion Eng. Design 58&59 (2001) 781.
[11] S. Jitsukawa, M. Tamura, B. van der Schaaf, R.L. Klueh, A. Alamo, C. Peterson, M. Schirra, G.R. Odette, A.-A.F. Tavassoli, K. Shiba, A. Kohyama, A. Kimura, J. Nucl. Mater. 307–311 (2002) 1057.
[12] A.-A.F. Tavassoli, RAFM Steels – Rules for design and Inspection, Annual report of the Association Euratom/CEA 2000, p. 235, with full Appendix A text available from EFDA, Garching, Germany.